© 2016. Published by The Company of Biologists Ltd | Journal of Cell Science (2016) 129, 1210-1222 doi:10.1242/jcs.181883

RESEARCH ARTICLE

Activator of G-protein signaling 8 is involved in VEGF-mediated signal processing during angiogenesis

Hisaki Hayashi, Abdullah Al Mamun, Miho Sakima and Motohiko Sato*

ABSTRACT

Activator of G-protein signaling 8 (AGS8, also known as FNDC1) is a receptor-independent accessory protein for the Gβγ subunit, which was isolated from rat heart subjected to repetitive transient ischemia with the substantial development of collaterals. Here, we report the role of AGS8 in vessel formation by endothelial cells. Knockdown of AGS8 by small interfering RNA (siRNA) inhibited vascular endothelial growth factor (VEGF)-induced tube formation, as well as VEGF-stimulated cell growth and migration. VEGF stimulated the phosphorylation of the VEGF receptor-2 (VEGFR-2, also known as KDR), ERK1/2 and p38 MAPK; however, knockdown of AGS8 inhibited these signaling events. Signal alterations by AGS8 siRNA were associated with a decrease of cell surface VEGFR-2 and an increase of VEGFR-2 in the cytosol. Endocytosis blockers did not influence the decrease of VEGFR-2 by AGS8 siRNA, suggesting the involvement of AGS8 in VEGFR-2 trafficking to the plasma membrane. VEGFR-2 formed a complex with AGS8 in cells, and a peptide designed to disrupt AGS8–Gβγ interaction inhibited VEGF-induced tube formation. These data suggest a potential role for AGS8–Gβγ in VEGF signal processing. AGS8 might play a key role in tissue adaptation by regulating angiogenic events.

KEY WORDS: Angiogenesis, VEGF, Endothelial cell, G protein, AGS protein

INTRODUCTION

Angiogenesis is the formation of new blood vessels from the existing vascular network, which is induced under physiological and pathophysiological stimuli, including hypoxia and ischemia, inflammation, wound healing and tumor genesis. Proliferation, tube formation and migration of endothelial cells are essential steps in the multiple processes of angiogenesis. Although various growth factors initiate downstream signaling pathways mediated by tyrosine kinase receptors, heterotrimeric G-proteins are also involved in signal integration in angiogenesis. Receptor tyrosine kinases, such as platelet-derived growth factor β receptor, insulin receptor and insulin-like growth factor receptor, use heterotrimeric G-proteins to mediate angiogenic signaling (Imamura et al., 1999; Alderton et al., 2001; Kuemmerle and Murthy, 2001). Additionally, $G\alpha_{q/11}$ and Gβγ subunits mediate vascular endothelial growth factor (VEGF)-mediated cell proliferation (Zeng et al., 2002, 2003). $G\gamma_2$ is required for VEGF-mediated angiogenesis in zebrafish (Leung et al., 2006).

G-protein signaling plays important roles in the maintenance of cell function under conditions of physiological stress. In the conventional model, heterotrimeric G-proteins are activated by G-protein-coupled receptors at the cell surface in response to extracellular stimuli. However, many studies indicate the existence of accessory proteins that directly regulate the activation status of heterotrimeric G-proteins without receptor activation. Such accessory proteins include proteins that activate or deactivate the Gα subunit or work as alternative binding partners for Gα or Gβγ subunits (Sato et al., 2006a; Kimple et al., 2011; Blumer and Lanier, 2014). This novel class of regulatory proteins might provide an alternative signal input through heterotrimeric G-protein signaling that is involved in various tissue responses to pathophysiological stress (Sato, 2013).

For example, dexamethasone-induced Ras-related protein 1 (DexRas1, also known as RASD1), a direct activator of $G\alpha_i$ subunits, is involved in the secretion of atrial natriuretic factor during volume overload in heart failure. Transcription factor E3 (TFE3, also known as AGS11), which was isolated from murine hypertrophied heart, selectively forms a complex with the $G\alpha_{16}$ subunit (Sato et al., 2011). TFE3–$G\alpha_{16}$ is associated with the induction of claudin-14 through an new type of transcriptional regulation (Sato et al., 2011). Regulators of G-protein signaling (RGSs), a family of proteins that accelerate the GTPase activity of the Gα subunit leading to inhibition of G-protein signaling, are involved in hypertension, cardiac hypertrophy and/or hypoxia-mediated injury (Wieland and Mittmann, 2003; Gu et al., 2009; Zhang and Mende, 2011). Interestingly, RGS5, which acts as a GAP for $G\alpha_q$ and $G\alpha_{i/o}$ subunits, is reported to be an important player in vascular remodeling. In particular, roles of RGS5 in pericytes and endothelial cells in neovascularization in tumors have been described (Nisancioglu et al., 2008; Silini et al., 2012).

Previously, we identified activator of G-protein signaling 8 (AGS8, also known as FNDC1) from a cDNA library of the rat heart subjected to repetitive transient ischemia (Sato et al., 2006b). AGS8 was upregulated in response to hypoxia and ischemia in the myocardium and interacted directly with Gβγ. Further analysis indicated that AGS8–Gβγ plays a pivotal role in the hypoxia-induced apoptosis of cardiomyocytes by regulating connexin 43 (CX43, also known as GJA1) permeability (Sato et al., 2009). The rat heart from which AGS8 was isolated had an extensive development of collateral vessels induced by repetitive transient ischemia (Sato et al., 2006b). AGS8 is also expressed in endothelial cells, which might be involved in angiogenic events (Sato et al., 2006b). However, the role of AGS8 in vessel formation has not been investigated. Here, we present the first report of the role of AGS8 in vessel formation, indicating that AGS8 is involved in angiogenic signaling in human umbilical vein endothelial cells (HUVECs).

RESULTS

Suppression of AGS8 attenuates tube formation of endothelial cells

To determine the role of AGS8 in vessel formation, we first analyzed the effect of knocking down AGS8 on tube formation

Department of Physiology, Aichi Medical University, Nagakute, Aichi 480-1195, Japan.

*Author for correspondence (motosato@aichi-med-u.ac.jp)

Received 28 October 2015; Accepted 26 January 2016

Journal of Cell Science (2016) 129, 1210-1222 doi:10.1242/jcs.181883

by HUVECs. Small interfering RNA (siRNA) for AGS8 (AGS8 siRNA), but not control siRNA, successfully suppressed the expression of AGS8 mRNA to 12.2% of the level observed in cells treated with control siRNA (Fig. 1A). At 48 h after siRNA treatment, HUVECs were subjected to a tube formation assay in Matrigel in the presence of 1% fetal bovine serum (FBS). AGS8 knockdown clearly inhibited tube formation at both time points analyzed, and the magnitude of inhibition was greater at 18 h (23.3±2.9% versus control) than at 6 h (51.7±4.3% versus control) (mean±s.e.m.; $P<0.01$; Fig. 1B). In separate experiments, we found that individual AGS8 siRNA significantly reduced the levels of AGS8 mRNA and tube formation by HUVECs (Fig. S1).

We also examined the influence of AGS8 knockdown on another type of endothelial cell: human umbilical arterial endothelial cells (HUAECs). As observed in HUVECs, AGS8 knockdown successfully inhibited tube formation to a similar extent at 6 h (38.5±6.8% versus control, $P<0.01$) and 18 h (30.0±4.8% versus control, $P<0.01$), suggesting that the effect of AGS8 was not specific to HUVECs (Fig. 1C).

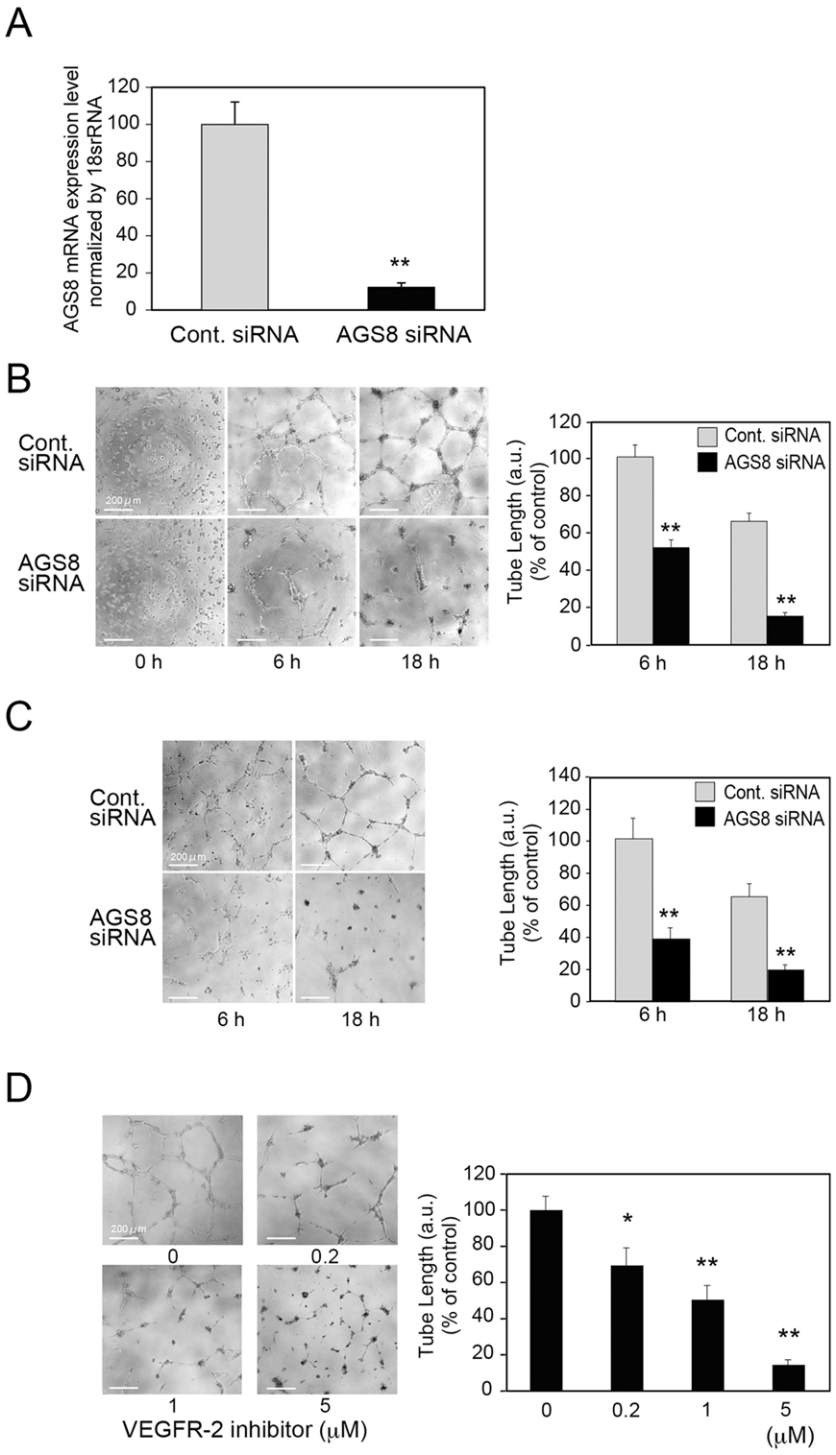

Fig. 1. Effect of AGS8 knockdown on serum-induced tube formation in endothelial cells. (A) HUVECs were transfected with control (Cont.) siRNA or AGS8 siRNA. After 48 h, AGS8 mRNA expression was determined by real-time PCR. Data are expressed as means±s.e.m. from seven independent experiments. $^{**}P<0.01$ (unpaired *t*-test). (B,C) At 48 h after transfection, HUVECs (B) or HUAECs (C) were subjected to a tube formation assay with 1% FBS as described in the Materials and Methods. Pictures were taken at indicated time points in independent microscopic field. Tube length in each image is presented in arbitrary units (a.u.), and expressed as the percentage of that with control siRNA at 6 h. Data are expressed as means±s.e.m. from four independent experiments performed in triplicate. $^{**}P<0.01$ versus control of each group (two-way ANOVA with Tukey's correction). (D) Effect of a VEGFR-2 kinase inhibitor on serum-induced tube formation. HUVECs were treated with 1% FBS and a VEGFR-2-specific inhibitor. Tube length in each image is presented as arbitrary units (a.u.), and expressed as a percentage of the value at for 0 μM. Data are means±s.e.m. from four independent experiments performed in triplicate. $^{*}P<0.05$, $^{**}P<0.01$ (one-way ANOVA with Dunnett's correction). Scale bars: 200 μm.

Journal of Cell Science (2016) 129, 1210-1222 doi:10.1242/jcs.181883

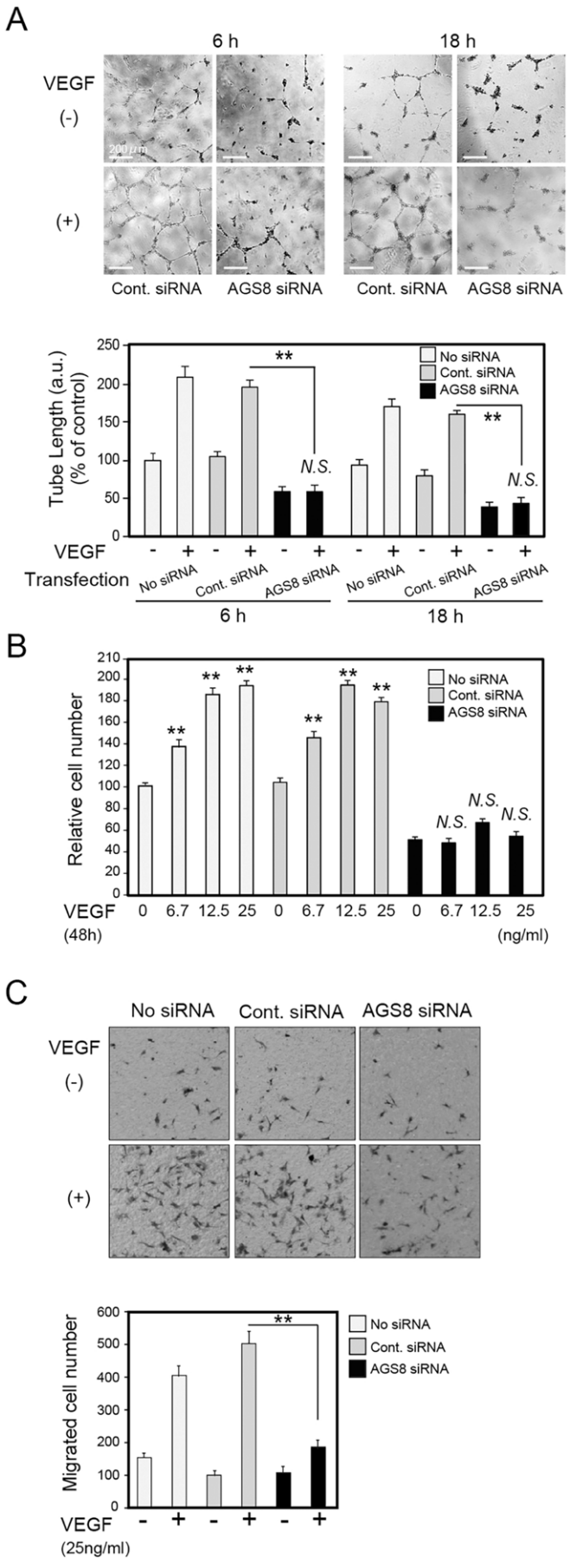

Fig. 2. Effect of AGS8 knockdown on VEGF-induced tube formation, cell proliferation and migration in HUVECs. (A) HUVECs transfected with control (Cont.) siRNA or AGS8 siRNA were subjected to a tube formation assay under stimulation with VEGF (25 ng/ml) as described in the Materials and Methods. Pictures were taken after 6 h and 18 h in independent microscopic fields. Tube length in each image is presented in arbitrary units (a.u.), and expressed as the percentage of that with control siRNA at 6 h. Data are expressed as means±s.e.m. from four independent experiments performed in triplicate. $^{**}P<0.01$ (two-way ANOVA with Tukey's correction). N.S., not significant (unpaired *t*-test). (B) HUVECs transfected with siRNA were seeded on 96-well plate, and incubated with EBM2 containing 1% FBS for 6 h. Then, cells were stimulated by VEGF for 48 h, and the viability of cells was determined by an MTT assay. Data are expressed as means±s.e.m. from four independent experiments performed in batches of six. The bar graph represents absorbance (*x*-axis, percentage of control) versus the VEGF concentration of each group (*y*-axis). $^{**}P<0.01$ or N.S. versus control of each group without VEGF treatment (one-way ANOVA with Dunnett's correction). (C) HUVECs on fibronectin-coated Transwell were stimulated with VEGF (25 ng/ml) for 4 h, then fixed with 4% PFA followed by staining with 1% Crystal Violet. The migrated cells were counted from three independent microscopic fields. Representative pictures are shown in the upper panel; migrated cell numbers are shown in the lower panel. Data are expressed as means±s.e.m. from four independent experiments performed in duplicate. $^{**}P<0.01$ (two-way ANOVA with Tukey's correction).

VEGF is one of the most important growth factors for vessel formation among pro-angiogenic substrates. Indeed, tube formation stimulated by FBS was blocked efficiently by a vascular endothelial growth factor receptor 2 (VEGFR-2, also known as KDR) kinase inhibitor in a dose-dependent manner (Fig. 1D). Next, we focused on the involvement of AGS8 in VEGF-mediated signaling in the following experiments.

AGS8 is involved in VEGF-mediated signaling in endothelial cells

VEGF (25 ng/ml) stimulated tube formation in HUVECs to a similar extent as 1% FBS (Fig. 2A). AGS8 knockdown again inhibited tube formation at 6 h (30.0±4.0% versus control) and at 18 h (27.0±4.8% versus control) (mean±s.e.m.; $P<0.01$; Fig. 2A). The influence of AGS8 knockdown on other VEGF-mediated cellular events was analyzed next for the growth and migration of cells. VEGF simulated cell growth in a dose-dependent manner. Control siRNA did not influence this proliferation; however, AGS8 siRNA completely blocked cell growth (Fig. 2B). The number of migrating cells was also increased following stimulation with VEGF in a dose-dependent manner. Control siRNA did not influence this activity; however, again, AGS8 siRNA completely blocked this effect (Fig. 2C). These data suggest that AGS8 is required for VEGF-mediated signaling in HUVECs.

Knockdown of AGS8 blocks VEGFR phosphorylation and intracellular signaling

The influence of AGS8 knockdown on VEGF-activated intracellular signaling was determined in HUVECs (Fig. 3A,B). VEGF increased the phosphorylation of p38 MAPK family proteins and ERK1 and ERK2 (ERK1/2, also known as MAPK3 and MAPK1, respectively) with a peak at 5–10 min (Fig. 3B). Knockdown of AGS8 did not influence the expression levels of both kinases; however, their phosphorylation was significantly reduced.

Six tyrosine residues of VEGFR-2, located in the kinase insert domain, distal kinase domain and C-terminal tail, are phosphorylated following binding of VEGF to its receptor (Roskoski, 2008). We examined the influence of AGS8 siRNA on the phosphorylation of each domain. Phosphorylation of VEGFR-2

Journal of Cell Science

Journal of Cell Science (2016) 129, 1210-1222 doi:10.1242/jcs.181883

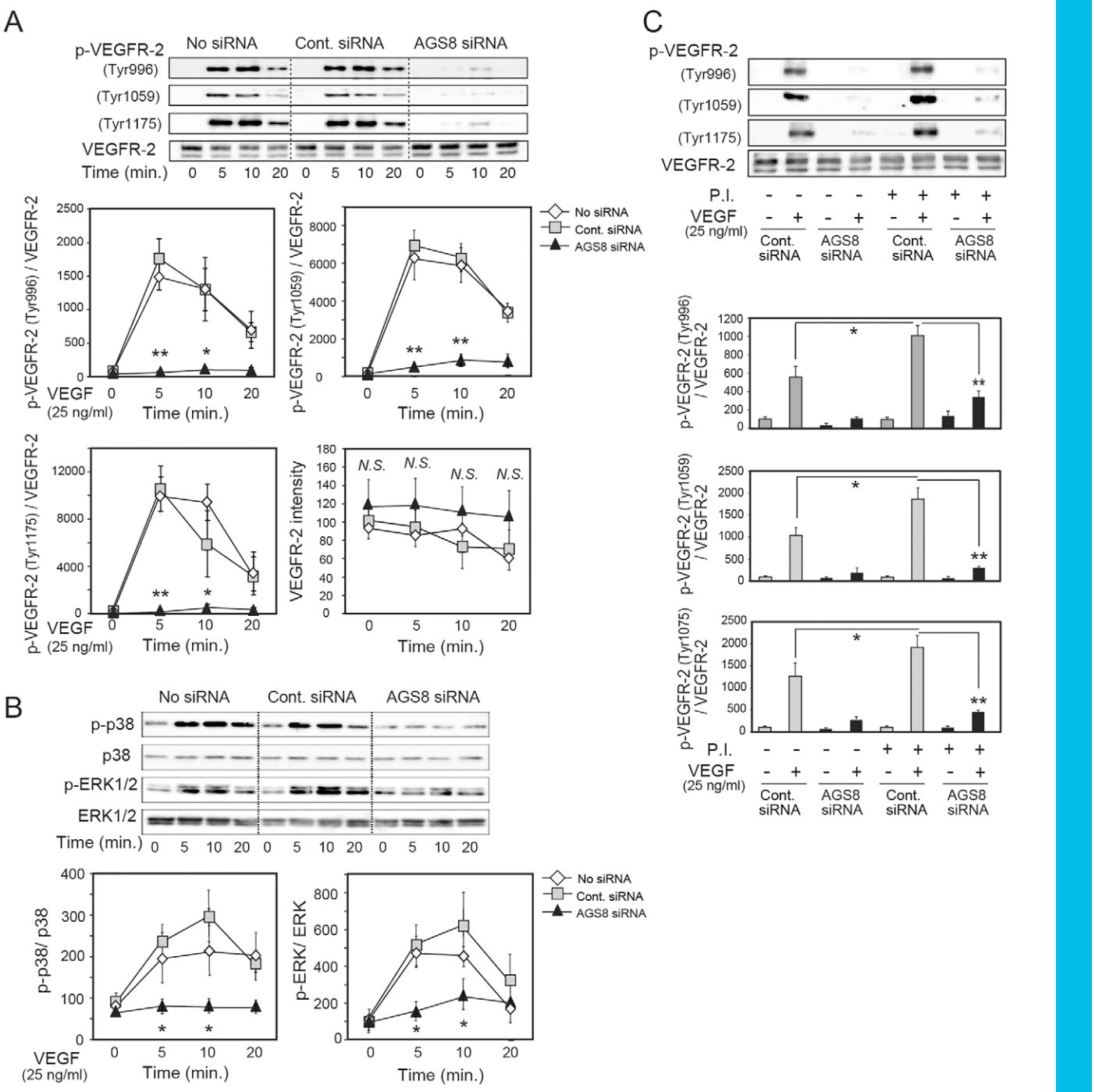

Fig. 3. Effect of AGS8 knockdown on VEGF-induced phosphorylation of VEGFR-2, p38 MAPK and ERK1/2. Immunoblot of phospho (p)-VEGFR-2 (A), and p-ERK1/2 and p-p38 MAPK (B). Cell lysate (10–20 µg) from HUVECs transfected with no siRNA, control (Cont.) siRNA or AGS8 siRNA was subjected to immunoblotting, and the intensity of signal was quantified by densitometric analysis. The value was normalized to that of VEGFR-2 (A), and ERK1/2 and p38 MAPK (B), respectively. Representative pictures are shown. **P*<0.05, ***P*<0.01 versus control siRNA (two-way ANOVA with Tukey's correction). (C) HUVECs transfected with the indicated siRNA were treated with phosphatase inhibitor (P.I.) for 30 min, then stimulated with VEGF (25 ng/ml) for 15 min. Immunoblotting was performed as A. Data are means±s.e.m. from four independent experiments. **P*<0.05, ***P*<0.01 (unpaired *t*-test).

was increased at a number of tyrosine residues; namely, Tyr996 in the kinase insert domain, Tyr1054 in the distal kinase domain, and Tyr1175 in the C-terminal tail, with a peak at 5–10 min; however, the phosphorylation of all tyrosine residues was significantly reduced following AGS8 knockdown (Fig. 3A). By contrast, the expression level of VEGFR-2 was not decreased by AGS8 siRNA, suggesting that AGS8 is required for VEGF-induced receptor phosphorylation.

Phosphatase inhibitors clearly increased the magnitude of phosphorylation of VEGFR-2 following VEGF stimulation (at Tyr996, 66.0±8.1%; Tyr1059, 80.1±5.3%; and Tyr1179, 51.2±4.0% versus the indicated relative control; mean±s.e.m., $P<0.05$). However, they only led to a partial recovery in the phosphorylation of VEGFR-2 upon AGS8 siRNA treatment, suggesting the effect of AGS8 siRNA was not due to an increase in phosphatase activity (Fig. 3C).

Journal of Cell Science (2016) 129, 1210-1222 doi:10.1242/jcs.181883

Influence of AGS8 knockdown on EGF, bFGF and NRP1

To determine whether AGS8 generally influences the signal processing of receptor tyrosine kinases, the effect of AGS8 siRNA on other transmembrane tyrosine kinase receptors was analyzed by stimulating cells with epidermal growth factor (EGF) and basic fibroblast growth factor (bFGF). Interestingly, AGS8 siRNA did not attenuate EGF-mediated cell proliferation or EGFR phosphorylation (Fig. 4A,B). Likewise, bFGF still stimulated cell proliferation in a dose-dependent manner following silencing of AGS8, whereas the response to 10 ng/ml bFGF was lower in the AGS8 siRNA group than in the control siRNA group (Fig. 4C). Overall, the effect of AGS8 siRNA on EGF and bFGF signaling was limited, suggesting the preferential regulation of VEGFR-2-mediated signaling by AGS8.

The neuropilin 1 (NRP1) co-receptor is an important partner for optimal VEGF signaling (Pellet-Many et al., 2008). In particular,

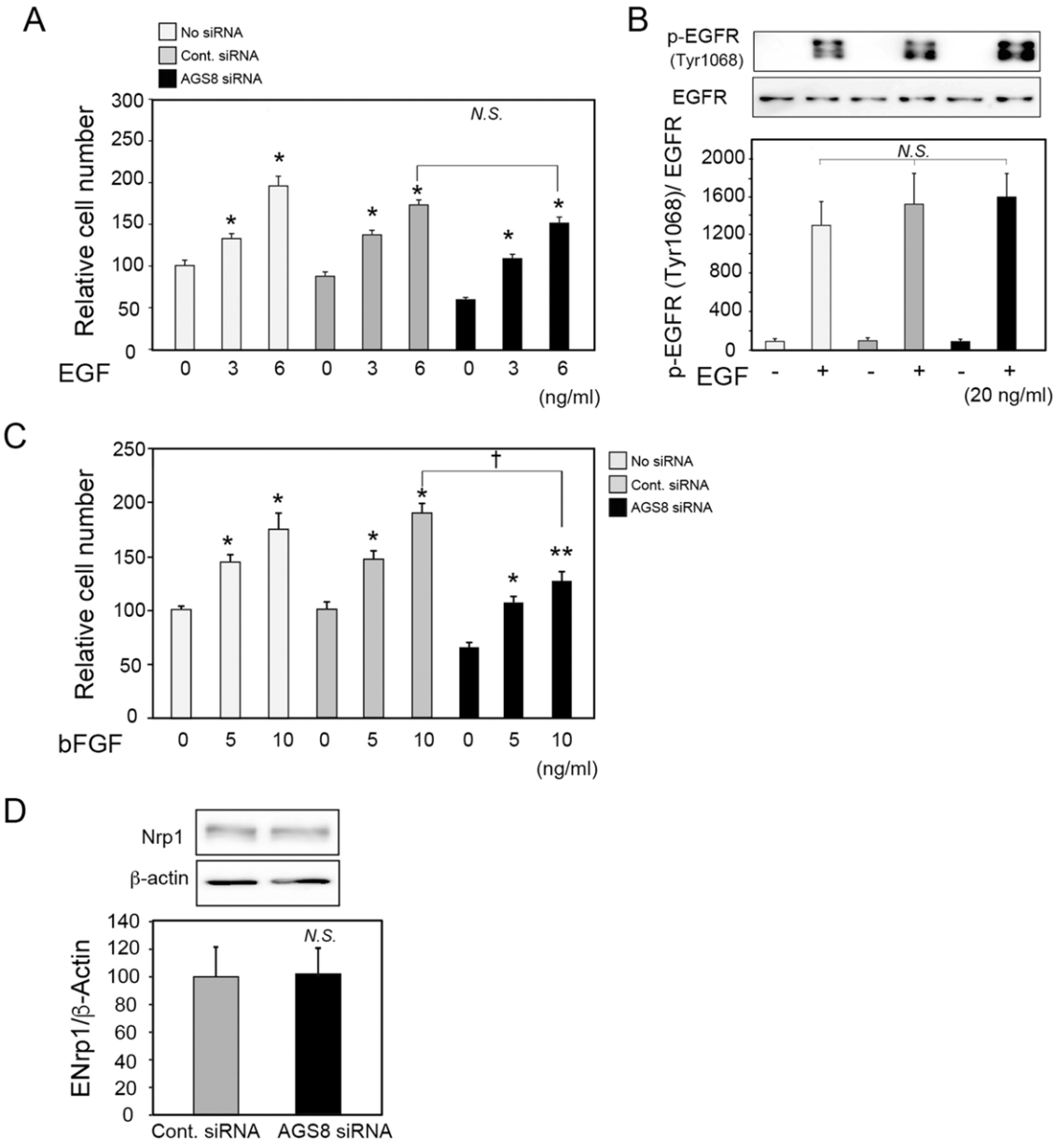

Fig. 4. Effect of AGS8 knockdown on EGF- or bFGF-mediated cellular events, and expression of neuropilin-1. (A) EGF-induced cell proliferation was determined by an MTT assay. HUVECs transfected with no siRNA, control (Cont.) siRNA or AGS8 siRNA were incubated with EGF for 24 h. Data are means± s.e.m. from four independent experiments performed in batches of six. The bar graph represents absorbance (*y*-axis, percentage of control) versus EGF concentration of each group (*x*-axis). **P*<0.05 (one-way ANOVA with Dunnett's correction). N.S., not significant (two-way ANOVA). (B) Phosphorylation of EGF receptor (Tyr1068) was determined by immunoblotting HUVEC lysate (10∼20 µg). Representative pictures are shown in upper panels. A quantification of signal intensity of phospho-EGFR to that of EGFR is presented in lower bar graph. Data are means±s.e.m. from four independent experiments. N.S. (two-way ANOVA). (C) bFGF-induced cell proliferation was determined using an MTT assay. siRNA-transfected HUVECs were incubated with bFGF for 48 h. Data are means±s.e.m. from four independent experiments performed in batches of six. The bar graph represents absorbance (*y*-axis, percentage of control) versus the bFGF concentration of each group (*x*-axis). **P*<0.05, ***P*<0.01 and N.S. (one-way ANOVA with Dunnett's correction); †*P*<0.05 (two-way ANOVA with Tukey's correction). (D) Expression of neuropilin-1 in AGS8 knockdown HUVECs was analyzed by immunoblotting. Representative images are shown in upper panel. The signal intensity of neuropilin-1 normalized to that of β-actin is presented in lower bar graph. Data are means±s.e.m. from four independent experiments. N.S. (unpaired *t*-test).

Journal of Cell Science

Journal of Cell Science (2016) 129, 1210-1222 doi:10.1242/jcs.181883

the NRP1–VEGFR-2 complex plays an important role in vascular formation and cardiovascular development (Pellet-Many et al., 2008). Knockdown of NRP1 reduced the expression of VEGFR-2 in endothelial cells (Holmes and Zachary, 2008); however, AGS8 siRNA did not influence the protein expression of NRP1 (Fig. 4D).

AGS8 mediates the cell surface expression of VEGFR

To investigate the mechanism by which AGS8 siRNA inhibited VEGFR signaling, we analyzed the level of cell surface VEGFR-2 using FACS analysis with an FITC-conjugated anti-VEGFR-2 antibody. Interestingly, VEGFR-2 was significantly decreased at the cell surface following treatment with AGS8 siRNA (37.9±4.8% versus control siRNA), whereas the level of VEGFR-2 was increased slightly in pearmeabilized cells (125.5±2.7% versus control siRNA) (mean±s.e.m., $P<0.01$; Fig. 5A). This was in contrast to the cell surface level of VEGFR-1 (also known as FLT1), which was increased following treatment with AGS8 siRNA (217±2.8% versus control siRNA, $P<0.01$), without changing the total expression level in cell (Fig. 5B).

Cell surface VEGFR-2 is known to be internalized upon its interaction with VEGF, which was detected by FACS analysis (45.0±4.4% versus control) (mean±s.e.m., $P<0.01$; Fig. 5C). The endocytosis blockers Pitstop and Dynasore successfully prevented the VEGF-induced decrease of cell surface VEGFR-2 (Fig. 5C). VEGFR-2 is also constitutively internalized and transferred to early endosomes (Jopling et al., 2011). The endocytosis blockers increased cell surface VEGFR-2 in the resting state without VEGF stimulation. However, they failed to lead to a recovery in the amount of VEGFR-2 upon AGS8 siRNA treatment, suggesting that the loss of cell surface receptors caused by AGS8 siRNA was not due to the acceleration of endocytosis (Fig. 5D).

Then, we examined the subcellular localization of VEGFR-2 using fluorescent immunostaining (Fig. 6). A proportion of VEGFR-2 was found in the Golgi during the resting state, as reported previously (Manickam et al., 2011). VEGFR-2 was also found in early endosomes, but was not detected in lysosomes. Interestingly, AGS8 knockdown increased the intracellular pool of VEGFR-2 in the Golgi and early endosomes, but not in lysosomes (Fig. 6). These data suggest that AGS8 is involved in VEGFR-2 trafficking from the Golgi to the cell surface, and in VEGFR-2 recycling through early endosomes.

AGS8 forms a protein complex with VEGFR-2 and Gβγ

Next, we determined whether AGS8 formed a protein complex with VEGFR-2 and Gβγ in cells. An Xpress-tagged C-terminal region of AGS8 (AGS8C), which binds to Gβγ, was transfected into COS7 cells with a combination of VEGFR-2, and Gβ and Gγ (Sato et al., 2009). Anti-VEGFR-2 antibody successfully immunoprecipitated AGS8C and/or AGS8C–Gβγ, but failed to isolate AGS8C from lysate in the absence of VEGFR-2 expression (Fig. 7A, left panel). Gβ itself was not co-immunoprecipitated with VEGFR-2 in the absence of AGS8C (Fig. 7A, right panel). In the reverse experiment, anti-Xpress antibody immunoprecipitated AGS8C with VEGFR-2, suggesting that AGS8C–Gβγ and VEGFR-2 are able to form a stable complex (Fig. 7A).

Previously, we identified the Gβγ interface of AGS8 and prepared a peptide (AGS8 peptide) based on the amino acids of the interaction domain between AGS8 and Gβγ (Sato et al., 2014). AGS8 peptide successfully blocked the association of Gβγ with AGS8 *in vitro* (Sato et al., 2014). Interestingly, the AGS8C–Gβγ signal co-immunoprecipitated with VEGFR-2 was decreased in the presence of AGS8 peptide (Fig. 7A, left panel). AGS8C was co-immunoprecipitated with VEGFR-2 in the absence of expressed Gβγ (Fig. 7A,B); however, AGS8 peptide did not influence co-immunoprecipitated AGS8C signal with VEGFR-2 (Fig. 7B, right two lanes). Conversely, AGS8 peptide decreased the signal of Gβγ co-immunoprecipitated with AGS8C (Fig. 7C). These data indicate that the AGS8 peptide interacts with the AGS8–Gβγ interface rather than with the AGS8–VEGFR-2 interface, and that the AGS8C-Gβγ interaction is important for the formation of a protein complex with VEGFR-2.

AGS8 peptide inhibits VEGF-induced tube formation

To determine the role of the AGS8–Gβγ complex in vessel formation, AGS8 peptide was delivered to HUVECs using a chemical reagent as described in the Materials and Methods. FACS analysis indicated that FITC-conjugated AGS8 peptide was incorporated successfully into HUVECs (Fig. 8A). Interestingly, AGS8 peptide inhibited tube formation in a dose-dependent manner (46.3±4.1% versus control, 20 μg/μl) (mean±s.e.m., $P<0.01$; Fig. 8B). As observed in AGS8-siRNA-treated HUVECs, AGS8 peptide inhibited the VEGF-mediated phosphorylation of VEGFR-2 (Fig. 8C). In contrast, with AGS8 peptide, gallein, which was designed to blocks universal Gβγ signaling, failed to inhibit VEGF-mediated tube formation, proliferation and VEGFR-2 phosphorylation (Fig. S2A–C) (Lehmann et al., 2008). The AGS8–Gβγ complex was not disrupted by gallein in cells (Fig. S2D). These data suggest that the AGS8–Gβγ complex, rather than a simple Gβγ signal input, is required by endothelial cells for the induction of angiogenesis.

DISCUSSION

Here, we first demonstrated the regulation of angiogenesis by an accessory protein for the heterotrimeric G-protein, AGS8. Knockdown of AGS8 in endothelial cells inhibited VEGF-mediated cellular events, including tube formation, migration and proliferation. AGS8 siRNA attenuated intracellular signaling, which was associated with a decrease of cell surface VEGFR-2. In contrast, AGS8 siRNA did not attenuate EGF- or bFGF-mediated cellular events. Expressed VEGFR-2 formed a protein complex with AGS8C in cells. Additionally, AGS8 peptide, which is designed to disrupt the interaction between AGS8 and Gβγ, blocked tube formation and VEGFR-2 phosphorylation. These observations suggest that the AGS8–Gβγ complex might be involved in angiogenic events under pathophysiological challenge and that AGS8 serves as a new regulatory pathway for vessel formation.

The importance of receptor-independent accessory proteins for heterotrimeric G-proteins in disease pathogenesis has been described in many studies (Sato, 2013). However, reports indicating roles for regulatory proteins of heterotrimeric G-proteins in vessel formation are very limited. The expression of RGS5, which binds to the $G\alpha_{i/o}$ and $G\alpha_{q}$ subunits (Zhou et al., 2001), has been reported in neovascular vessels. RGS5 is expressed in pericytes and is involved in neovascularization by regulating the maturation of pericytes (Nisancioglu et al., 2008). Additionally, RGS5 is highly expressed in endothelial cells isolated from human cancers, suggesting a role in the maintenance of a pro-angiogenic microenvironment (Silini et al., 2012). However, the specific pathway by which RGS5 influences vessel formation has not been well defined. AGS8 is clearly involved in angiogenic events that are mediated by regulating VEGF-mediated signaling. An AGS8–Gβγ blocking peptide inhibited this process, suggesting that the interaction of AGS8 with the Gβγ subunit is required for this process. Although the AGS8 peptide might influence AGS8–Gβγ

Journal of Cell Science (2016) 129, 1210-1222 doi:10.1242/jcs.181883

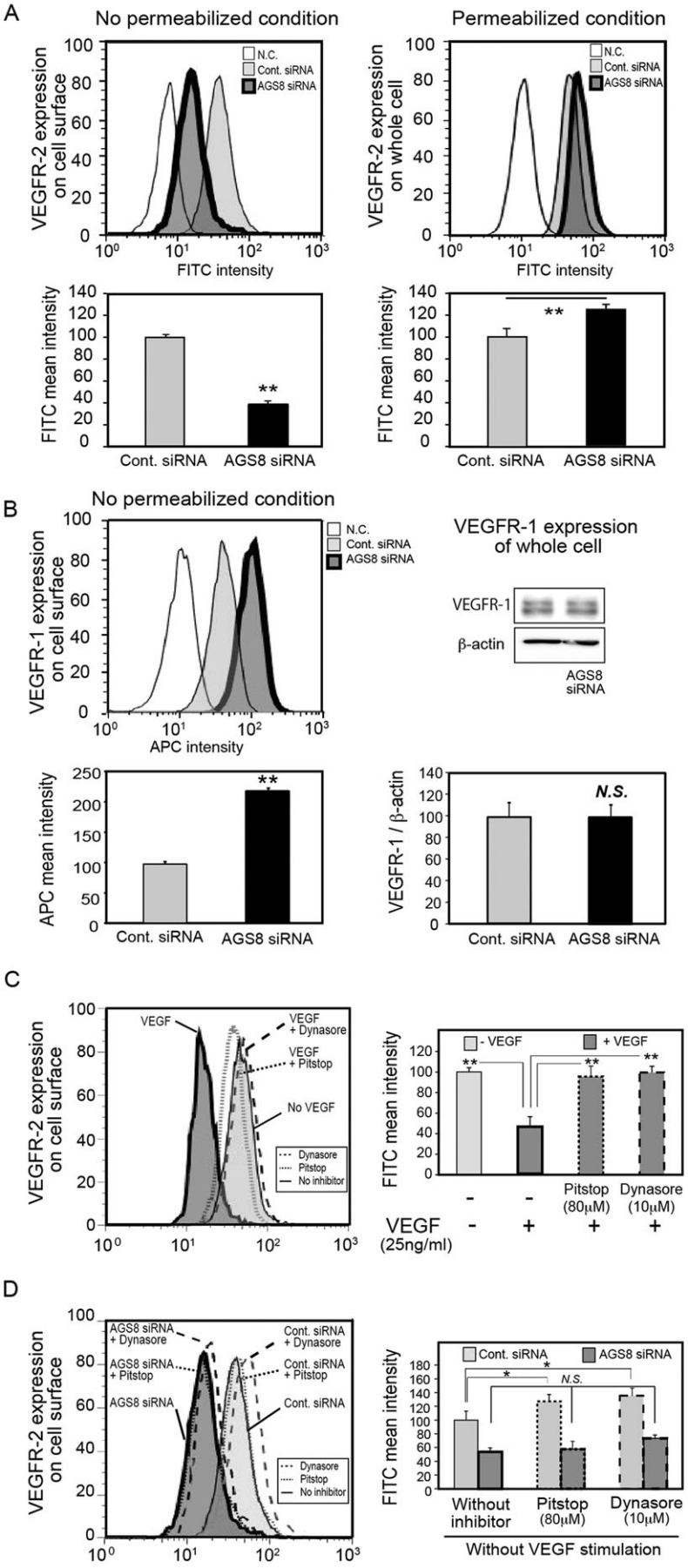

Fig. 5. Effect of AGS8siRNA on expression of VEGF receptors. HUVECs transfected with control (Cont.) siRNA or AGS8 siRNA were treated with FITC-conjugated VEGFR-2 with (A, right panel) or without (A, left panel) permeabilization, or APC-conjugated VEGFR-1 specific antibodies (B). Flow cytometric analysis was performed as described in the Materials and Methods. The histograms represent cell counts (*x*-axis, linear scale) versus FITC (A) or APC (B, left) intensity (*y*-axis, log scale). N.C. indicates negative control HUVECs treated with respective isotype human IgG labeled with FITC (A) or APC (B). Fluorescence mean intensity obtained from upper histograms were quantified and shown in bar graphs (lower panels). Data are mean±s.e.m. from four independent experiments. $^{**}P<0.01$ (unpaired *t*-test). (B) Right, immunoblot of VEGFR-1 in whole cell lysate. A representative picture from four independent experiments is shown. Quantification of signal intensity of VEGFR-1 was normalized to that of β-actin. $^{**}P<0.01$, N.S., not significant (unpaired *t*-test). (C,D) Effect of endocytosis inhibitors on expression of VEGFR-2 at the cell surface. (C) Upper panel, HUVECs were treated with Pitstop or Dynasore at indicated concentration for 30 min and stimulated by VEGF for 15 min, and expression of VEGF receptors at cell surface were determined by flow cytometric analysis. (C) Lower panel, fluorescence mean intensity from upper histograms were quantified. Fluorescence mean intensity obtained from upper histograms were shown in the lower panel. Data are means±s.e.m. (n=4); $^{**}P<0.01$ (one-way ANOVA with Tukey's correction). (D) Upper panel, AGS8-siRNA-transfected HUVECs were treated with Pitstop or Dynasore, and flow cytometric analysis was performed. (D) Lower panel, fluorescence mean intensity from upper histograms was quantified. Data are means±s.e.m. (n=4); *N.S.* (one-way ANOVA).

Journal of Cell Science

Journal of Cell Science (2016) 129, 1210-1222 doi:10.1242/jcs.181883

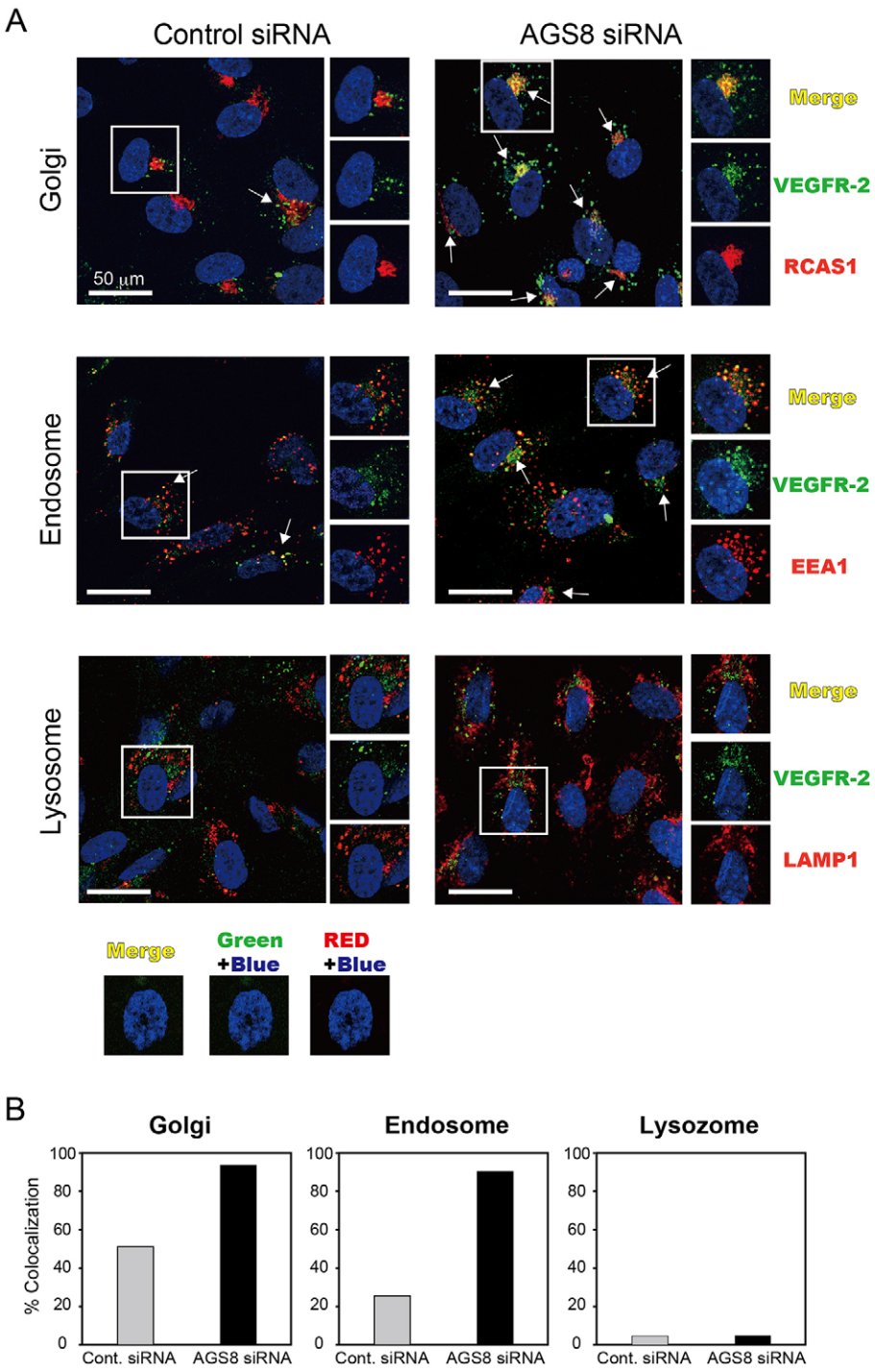

Fig. 6. Effect of AGS8 knockdown on intracellular distribution of VEGFR-2. (A) The intracellular distribution of VEGFR-2 was determined by fluorescent immunostaining as described in the Materials and Methods. HUVECs transfected with control siRNA or AGS8 siRNA were stained with VEGFR-2–FITC (green), anti-RCAS1 (Golgi marker, red), anti-EEA1 (endosome marker, red), anti-LAMP1 (lysosome marker, red), and DAPI (nuclei, blue). The area indicated with a square is shown in the right column. Scale bars: 50 μm. The arrows indicate cells in which VEGFR-2 colocalized and other organelles. (A) Lower panel, immunostaining with antibodies for negative controls. Cells were treated with FITC-conjugated anti-mouse-IgG antibody (green), an isotype control for anti-human-VEGFR-2–FITC, and Alexa-Fluor-594-conjugated anti-rabbit-IgG antibody (Red), common controls for anti-RCAS1, EEA1 and RAMP1 rabbit antibodies, together with DAPI (blue). (B) The number of cells, in which VEGFR-2 and other organelles colocalized, was counted in about 100 transfected cells from four or five independent experiments. Cont. siRNA, control siRNA.

outside of being in a complex with VEGFR-2, and the role of Gβγ in the VEGFR-2–AGS8–Gβγ complex is not completely defined, the current data suggest the potential importance of the AGS8–Gβγ complex in the regulation of cellular functions.

We found that AGS8 is involved in the intracellular distribution and/or trafficking of VEGFR-2. A previous report has indicated that 25% of VEGFR-2 is located in the Golgi complex and then recruited to the plasma membrane upon VEGF stimulation (Manickam et al., 2011). Additionally, VEGFR-2 undergoes constitutive endocytosis and recycling (Jopling et al., 2011). Endocytosis blockers prevent the loss of VEGFR-2 from the plasma membrane and lead to an increase of cell surface receptors (Gourlaouen et al., 2013). However, the decrease in VEGFR-2 caused by AGS8 siRNA was not rescued with endocytosis blockers, suggesting that AGS8 is involved in the trafficking of receptors toward the membrane rather than receptor endocytosis.

Interestingly, AGS8 knockdown had a limited effect on EGF or bFGF signaling, indicating the specificity of AGS8-mediated trafficking. Rab4, Rab5, Rab7 and Rab11 vesicles are reportedly involved in VEGFR-2 recycling (Jopling et al., 2009, 2014; Ballmer-Hofer et al., 2011). These Rab proteins are generally utilized in the recycling and/or degradation of various proteins, including EGFR (Ceresa, 2006). The preference of the AGS8 to

Journal of Cell Science (2016) 129, 1210-1222 doi:10.1242/jcs.181883

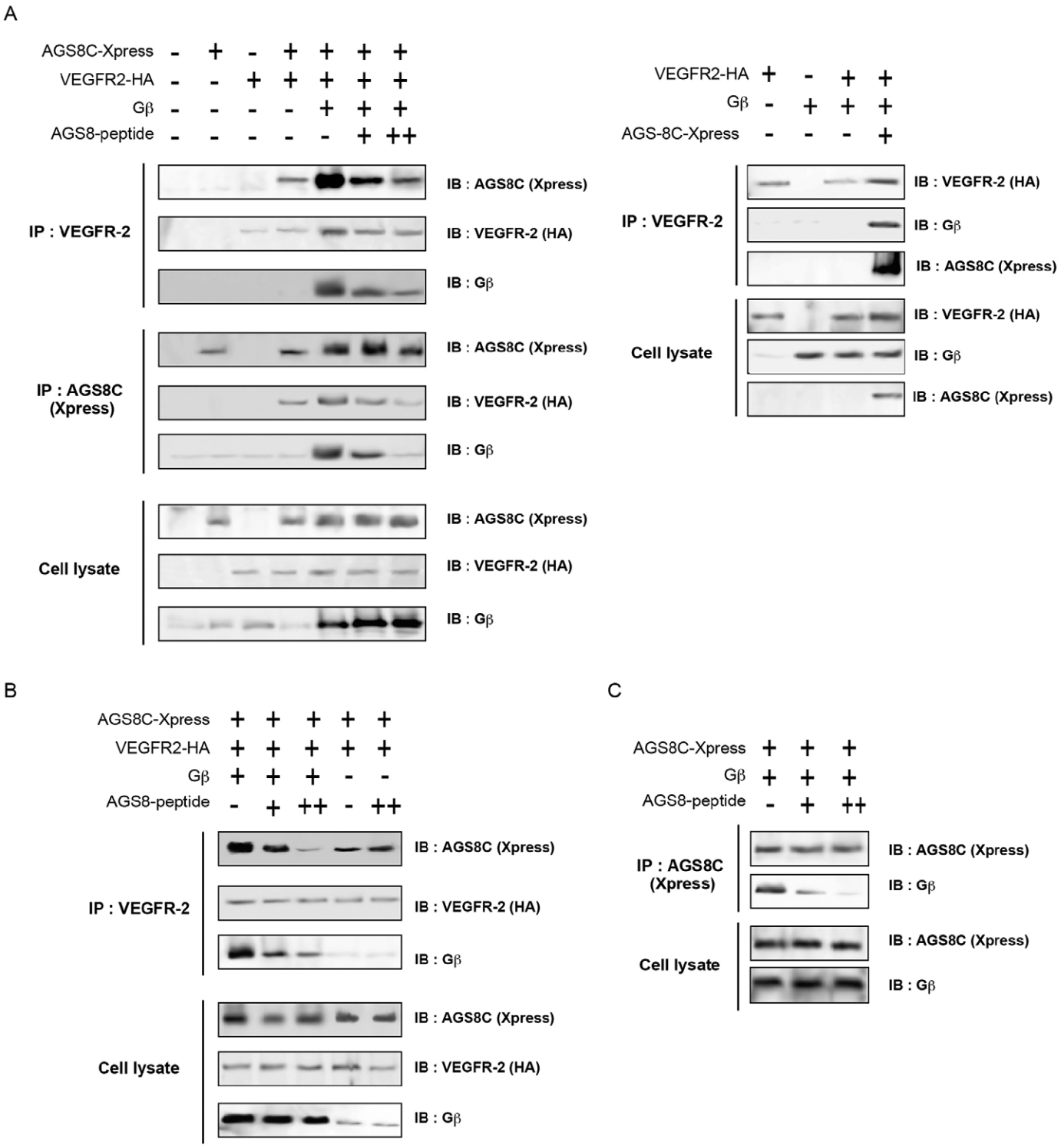

Fig. 7. Interaction of the C-terminal of AGS8 (AGS8-C) with VEGFR-2 and/or the Gβγ subunit. COS7 cells in a 100-mm dish were transfected with a combination of pcDNA3, pIREShrGFP2a::VEGFR-2 containing HA epitope tag (6 µg/dish), pcDNAHis::AGS8-C containing Xpress epitope tag (6 µg/dish), pcDNA3::$G\beta_1$ (3 µg/dish), pcDNA3::$G\gamma_2$ (3 µg/dish), and 2.4 (indicated as '+') or 12.0 (indicated as '++') µg of AGS8 peptide. The amount of DNA transfected was adjusted to 18 µg per dish with the pcDNA3 vector. Preparation of cell lysates and immunoprecipitation (IP) were performed as described in the Materials and Methods. The transferred membrane was reprobed with the antibodies (IB) indicated in the figure. These data are representative of five independent experiments with similar results.

modulate a specific receptor suggests that AGS8 is not involved directly in the function of Rab proteins; AGS8 might provide the specificity of trafficking by supporting the entry of VEGFR-2 to Rab vesicles.

Although ~40% of VEGFR-2 was still expressed at the membrane upon AGS8 siRNA treatment, phosphorylation of VEGFR-2 was clearly blocked by AGS8 siRNA. The reduction of cell surface VEGFR-2 might not fully explain the block of

Journal of Cell Science (2016) 129, 1210-1222 doi:10.1242/jcs.181883

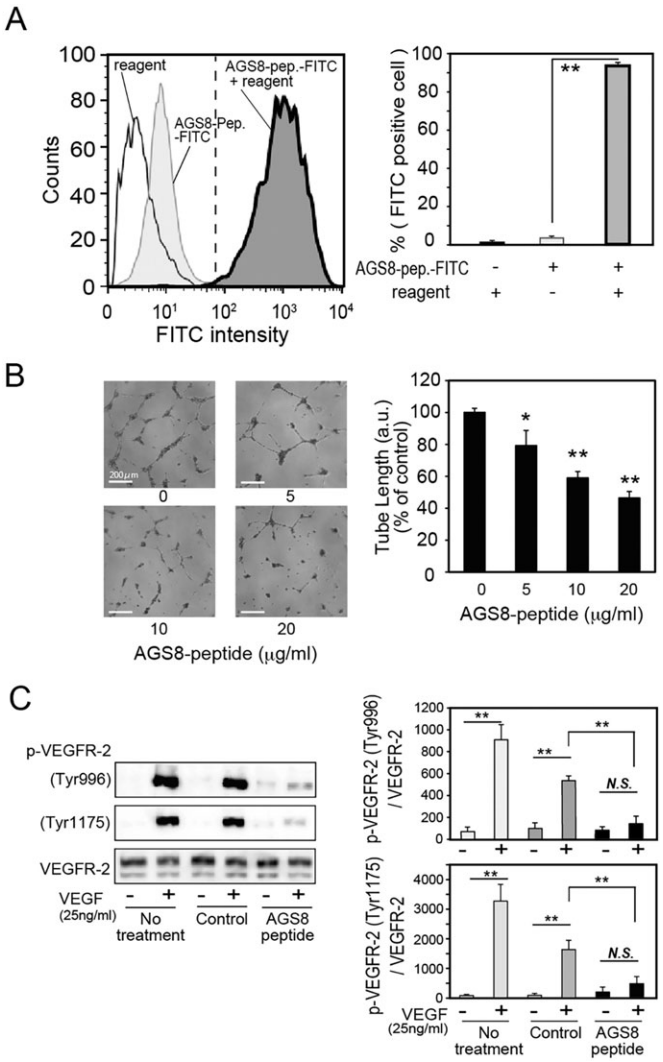

Fig. 8. Effect of AGS8 peptide on VEGF-induced tube formation and VEGFR-2 phosphorylation. (A) The efficiency of peptide uptake in HUVECs was analyzed by flow cytometry. AGS8-peptide conjugated to FITC (AGS8-Pep.–FITC) was introduced into HUVECs using a transfection reagent (reagent) as described in the Materials and Methods. A FITC intensity greater than 7.0×10^2 (indicated by the dashed line) was recognized as FITC positive. Data are means±s.e.m. of four independent experiments. $^{**}P<0.01$ (unpaired *t*-test). (B) AGS8 peptide was introduced into HUVECs by delivery reagent as described in the Materials and Methods. Tube length in each image is presented in arbitrary units (a.u.), and expressed as a percentage the result for the control without AGS8 peptide. Data are means±s.e.m. from four independent triplicate experiments. $^{**}P<0.01$, $^{*}P<0.05$ (one-way ANOVA with Dunnet's correction). (C) AGS8 peptide (2.0 μg/35-mm dish) was delivered into HUVECs, and cells were stimulated with VEGF (25 ng/ml) for 5 min. Cell lysates were subjected to immunoblotting with antibody against phospho (p)-VEGFR-2 (Tyr996, Tyr1175). Representative immunoblot images are shown (left panel). Signal intensity of phospho-VEGFR-2 was quantified (right panels). The data are means±s.e.m. (n=4). $^{**}P<0.01$; N.S., not significant (unpaired *t*-test).

VEGF-mediated signaling. VEGFR-2 dephosphorylation is regulated by multiple protein tyrosine phosphatases (PTPs), including density-enhanced phosphatase 1, PTPβ and PTP-1B (also known as PTPRJ, PTPRB and PTPN1, respectively) (Kappert et al., 2005). The decreased VEGFR-2 phosphorylation upon AGS8 siRNA expression was not repressed by phosphatase inhibitors, suggesting that AGS8 is not involved in the regulation of phosphatases.

Cell surface VEGFR-2 was decreased following AGS8 siRNA knockdown, whereas VEGFR-1 was increased. The counterbalanced expression of VEGFR-1 and VEGFR-2 in endothelial cells has been reported during hypoxia (Marti and Risau, 1998; Ulyatt et al., 2011), ischemia (Imoukhuede et al., 2013) and VEGF treatment (Imoukhuede and Popel, 2011). VEGFR-1 is an isoform with higher VEGF affinity but less kinase activity than VEGFR-2, suggesting a decoy function for VEGFR-1 by sequestering VEGF (Roskoski, 2008). The level of VEGFR-1 in the plasma membrane is up to 10-fold less than that of VEGFR-2 (Imoukhuede and Popel, 2011). A proportion of VEGFR-1 forms heterodimers with abundant VEGFR-2, which inhibits some VEGFR-2-mediated functions (Cudmore et al., 2012). A decrease of VEGFR-2 homodimers and increase of VEGFR-1–VEGFR-2 heterodimers might contribute to the anti-angiogenic effect of AGS8 siRNA.

Our serial observations indicate the important roles of AGS8–Gβγ in multiple cellular events. AGS8 is a Gβγ-interacting protein isolated from a rat heart with a substantial development of collaterals following repetitive transient ischemia (Sato et al., 2006b). In endothelial cells, AGS8 is essential for VEGF-mediated vessel formation, particularly the appropriate distribution of VEGFRs. In cardiomyocytes, AGS8 is involved in hypoxia–ischemia-induced apoptosis by regulating the localization and permeability of the cell surface channel protein CX43 (Sato et al., 2009). Both cellular events are blocked by the AGS8 peptide, which disrupts the interaction of AGS8 with Gβγ (Sato et al., 2014). These data might suggest a potential role for AGS8–Gβγ in the intracellular trafficking of specific proteins.

Here, we demonstrated a new regulation of vessel formation through a receptor-independent G-protein. Given that AGS8 was isolated from a rat heart subjected to repetitive transient ischemia with the development of collaterals, AGS8 likely plays key roles in pathophysiological responses in the myocardium, particularly in cardiomyocytes and endothelial cells. Accessory proteins for this heterotrimeric G-protein are involved in disease development and are potential targets for drug discovery.

MATERIALS AND METHODS

Materials

Pre-designed double-strand siRNA oligonucleotides to human AGS8 (stealth siRNAs, set of three; HSS150034, HSS150035, HSS189126), siRNA negative control with scrambled sequences, anti-Xpress mouse monoclonal antibody (#R910-25, 1:5000 dilution for immunoblot, 1:100 dilution for immunoprecipitation) and Lipofectamine siRNA Max reagent were purchased from Life Technologies (Carlsbad, CA). Antibodies against VEGFR-1 (#2893, 1:1000 dilution), VEGFR-2 (#2479, 1:1000 dilution for immunoblot, 1:100 dilution for immunoprecipitation), phospho-VEGFR-2 [Tyr996 (#2474, 1:1000 dilution), Tyr1059 (#3817, 1:1000 dilution) and Tyr1175 (#3770, 1:1000 dilution)], p38MAPK family proteins (#9212, 1:1000 dilution), phospho-p38 MAPK family proteins (Thr180/Tyr182) (#9211, 1:1000 dilution), ERK1/2 (p44/42) MAPK (#9102, 1:1000 dilution), phospho-ERK1/2 (p44/42) MAPK (Thr 202/204) (#9101, 1:1000 dilution), EGFR (#2232, 1:1000 dilution), phospho-EGF (Tyr1068) (#2234, 1:1000 dilution), anti-EEA1 (C45B10) (#3288, 1:200 dilution), anti-LAMP1(D2D11) (#9091, 1:200 dilution) and anti-RCAS1 (D2B6N) (#12290, 1:200 dilution) were purchased from Cell Signaling Technology (Danvers, MA). Anti-neuropilin-1 antibody was from Novus Biologicals (NBP1-40666, Littleton, CO; 1:1000 dilution). Anti-HA antibody (12CA5, 1:100 dilution) and β-actin antibody (AC-74, 1:5000 dilution) were from Sigma-Aldrich (St. Louis, MO). Anti Gβ subunit antibody (#SC-378, 1:1000 dilution) was purchased from Santa Cruz Biotechnology (Dallas, TX). pIRESHA-VEGFR-2 was kindly provided by Jacques Huot and François Houle (Centre de recherche en cancérologie de l'Université Laval, Québec, Canada) (Lamalice et al., 2006).

Journal of Cell Science (2016) 129, 1210-1222 doi:10.1242/jcs.181883

Cell culture and siRNA transfection

Human umbilical vein endothelial cells (HUVECs) and human umbilical artery endothelial cells (HUAECs), were cultured in endothelial cell growth medium (EGM)-2 (Lonza, Basel, Switzerland) or endothelial cell growth medium on fibronectin-coated (Sigma-Aldrich) culture dish or plate (Corning, Schiphol, The Netherlands). For siRNA transfection, cells were incubated in six-well plates and treated with three sets of each 40 nM Stealth siRNAs or negative control with Lipofectamine siRNA Max according to the manufacturer's instruction. AGS8 mRNA expression was determined by real-time PCR (Sato et al., 2009). The primers for RT-PCR were as follows: human AGS8, forward, 5′-TTCCGTAACCCTCTCTCCCG-3′; reverse, 5′-AACCCACGATCAAGGTCCAC-3′. Each AGS8 siRNA significantly reduced the level of AGS8 mRNA (H.H. and M.S., unpublished observation).

COS-7 were cultured and transfected as described previously (Sato et al., 2011). In brief, cells were suspended at $0.5–1.0\times10^5$ cells/ml, and 10 ml of suspension was plated in 100-mm dishes. After 18 h, cells were transfected with 18 µg of cDNA with Lipofectamine 3000 (Life Technologies) according to the manufacturer's instruction. Cell lysis and fractionation were performed as described previously (Sato et al., 1995, 2004).

Tube formation assay

Growth-factor-reduced Matrigel (BD Biosciences, San Jose, CA) was used to coat the 96-well plates (50 µl/well), which was then allowed to polymerize at 37°C for 1 h. Cells were incubated with endothelial cell basal medium (EBM)-2 (Lonza) containing 1% fetal bovine serum (FBS) for 6 h, and were then trypsinized and suspended in 250 µl of EBM-2 containing 1% FBS. Cells were seeded at 1×10^4 cells/well onto Matrigel and further incubated. In some experiments, cells were treated with VEGF at 25 ng/ml or VEGFR-2 inhibitor (R&D Systems, Minneapolis, MN) at 0.1 to 5 µM, a Gβγ inhibitor gallein (Millipore, Billerica, MA) at 3.3 to 30 µM, or AGS8-blocking peptide (Sato et al., 2014) at 100 µg/ml. Pictures of capillary-like structures were taken at 6-h and 18-h time points. Tube length was determined by tracing lines along the cells using ImageJ software (Schneider et al., 2012). The total tube length of each image was determined by an observer blinded to the conditions. The data are presented in arbitrary units (a.u.).

MTT assay

Human recombinant VEGF, epidermal growth factor (EGF) and basic fibroblast growth factor (bFGF) were purchased from Wako Chemicals (Osaka, Japan). The cell proliferation was analyzed using a Vybrant MTT cell proliferation assay kit (Life Technologies), according to the product instructions. Briefly, cells in six-well plates were transfected with siRNAs and incubated for 24 h. Next, cells were transferred to 96-well plates at 5×10^3 cells/well. After 24 h, cells were incubated with EBM-2 containing 1% FBS for 6 h, and treated with VEGF for 48 h, EGF for 24 h or bFGF for 48 h. Then, cells were incubated with MTT at 37°C for 4 h. Medium was removed, and SDS-HCl solution (10% SDS, 0.01 M HCl) was added to each well. After incubation for 18 h at 37°C, the absorbance was measured with a SpectraMax (Molecular Devices) at a wavelength of 570 nm.

Cells migration assay

HUVECs suspended at 5×10^4 cells/200 µl were seeded on fibronectin-coated Transwell inserts with 8 µm pores (BD Biosciences) that had been pretreated with 3% BSA. Cell migration was stimulated by VEGF (25 ng/ml) in the lower chamber of the 24-well plate. After 4 h, the Transwell inserts were fixed in 4% PFA, stained with 1% Crystal Violet. Digital microscopic images of the underside of each Transwell insert at independent microscopic fields were taken, and cells stained were counted.

Peptide delivery

Delivery of peptide to cells was essentially performed as described previously (Sato et al., 2014). Briefly, peptide was incubated with 4 µl of PLUSin (Polyplus, Illkirch, France) in 100 µl of EBM-2 for 15 min, and then the mixture was added to each well of cultured HUVECs in 12-well plates. Cells were then incubated for 4 h before stimulation by VEGF (25 ng/ml) for tube formation assay or immunoblotting. The incorporation of the peptide by cells was determined with fluorescein isothiocyanate (FITC)-conjugated AGS8 peptide by flow cytometric analysis (Sato et al., 2014). In some immunoprecipitation experiments, 2.4–12.0 µg of AGS8 peptide was incubated with 12 µl of Lipofectamine 3000 (Life Technologies) for 5 min, and then added the mixture to COS7 cells in a 10-cm dish 4 h before harvesting.

Immunoblotting

HUVECs were cultured in six-well plates were washed with ice-cold PBS, and collected in SDS-PAGE sample buffer (65.8 mM Tris-HCl, pH 6.8, 2.1% SDS, 26.3% glycerol, 0.01% Bromophenol Blue) with protease inhibitor cocktail (Roche, Indianapolis, IN) and 4% 2-mercaptoethanol. The lysates were separated by SDS-PAGE, and the gel was transferred onto the PVDF membrane (Millipore, Billerica, MA). The membrane was blocked with Tris-buffered saline containing 5% bovine serum albumin (Sigma-Aldrich) and incubated with primary antibodies. The membranes were then treated with horseradish-peroxidase-conjugated secondary antibodies (GE Healthcare, Munich, Germany), and signals were detected using Immunostar LD western blotting detection reagents (Wako Chemicals, Osaka, Japan) and a LAS4000 image analyzer (GE Healthcare). For quantification, the band intensity was analyzed by the ImageJ software.

Immunocytochemistry

HUVECs were cultured on the 13-mm poly-L-lysine-coated coverslips (Matsunami Glass, Osaka, Japan). Cells were washed twice with PBS, and then fixed with 4% paraformaldehyde containing 4% sucrose in PBS for 15 min followed by incubation with 0.2% Triton X-100 in PBS for 5 min. After three washes with PBS, cells were incubated with 5% normal donkey serum in PBS for 1 h to block the nonspecific staining, incubated with fluorescein-conjugated anti-human VEGFR-2 antibody (1:200 dilution; FAB357F, R&D Systems, Minneapolis, MN) and antibodies for organelles for 18 h at 4°C. Cells were incubated with DAPI (Life Technologies) in PBS for 5 min. Slides were then mounted with glass coverslips with Fluoro Keeper antifade reagent (Nacalai Tesque, Kyoto, Japan) or ProLong antifade Gold (Life Technologies). Images were obtained with a laser confocal microscope, LSM710 (Carl Zeiss, Jena, Germany).

Flow cytometric analysis

Fluorescence-activated cell sorting (FACS) was performed using a FACS Canto II (BD Biosciences, San Jose, CA). Cells were washed with PBS and detached from culture plate with Accutase (Innovative Cell Technologies, San Diego, CA), then fixed with 2% PFA for 30 min. In the experiments using permeabilization, the cells were incubated with 90% methanol on ice for 30 min. Cells were washed with PBS containing 1% FBS, and labeled with fluorescein-conjugated anti-human VEGFR-2 antibody (1:100 dilution) and allophycocyanin (APC)-conjugated anti-VEGFR-1 antibody (1:100 dilution; FAB321A, R&D Systems, Minneapolis, MN), fluorescein-conjugated IgG1 isotype control (1:100 dilution; IC002F, R&D Systems, Minneapolis, MN) or IgG1 APC-conjugated isotype control (1:100 dilution; IC002A, R & D Systems, Minneapolis, MN) for 1 h in the dark on ice. In some experiments, cells were treated with Pitstop (Abcam, Cambridge, MA, USA) or Dynasore (Sigma-Aldrich) for 30 min, then stimulated with VEGF (25 ng/ml) for 15 min before collecting cells. FACS Calibur and CellQuest software (BD Biosciences) was used for flow cytometric analysis and for data acquisition, respectively. Flow Jo (TreeStar, Ashland, OR, USA) was used for data analysis.

Immunoprecipitation

Cell lysates were prepared in 500 µl immune precipitation buffer [50 mM Tris-HCl pH 7.4, 70 mM NaCl, 5 mM EDTA, 1% IGEPAL CA-630 (Sigma), protease inhibitor cocktail (Complete Mini; Roche Applied Science)]. At total of 500–800 µg of lysate were incubated with 1.0–6.0 µg antibody for 18 h after pre-clearing with 25 µl of 50% Sepharose-G for 1 h at 4°C. The samples were incubated with 25 µl of 50% Sepharose-G for 1 h at 4°C, and the pellets were washed three times with the immune precipitation buffer. Proteins were eluted in 30 µl of 2× Laemmli buffer and resolved by SDS-PAGE (Sato et al., 2009).

Other procedures and data analysis

Other procedures were as previously described (Sato et al., 2009, 2011). Data are expressed as means±s.e.m. from independent experiments. Statistics were performed using a unpaired *t*-test or one-way or two-way ANOVA with Dunnett's or Tukey's correction as indicated in figure legends. All statistical analyses were performed with IBM SPSS software.

Acknowledgements

We thank Jacques Huot and Dr François Houle (Centre de recherche en cancérologie de l'Université Laval, Québec, Canada) for providing pIRESHA-VEGFR-2. We are also grateful to Hiroko Suzuki and Rie Takahashi for their technical assistance.

Competing interests

The authors declare no competing or financial interests.

Author contributions

M.S. conceived and coordinated the study and wrote the paper. H.H. designed and performed the study, and wrote the paper. A.A.M. and M.S. provided substantial technical assistance and contributed to the preparation of the figures. All authors analyzed the results and approved the final version of the manuscript.

Funding

This study was supported by a Grant-in-Aid for Scientific Research on Innovative Areas from Japan Society for Promotion of Science (JSPS) [grant number 25136721 to M.S.]; and a Grant-in-Aid for Scientific Research from Japan Society for Promotion of Science (JSPS) [grant number 24590280 to M.S.]; The Naito Foundation (to M.S.); DAIKO Foundation (to M.S.); the Takeda Science Foundation (to H.H.); and a Strategic Research Foundation Grant-aided Project for Private Universities from the Ministry of Education, Culture, Sports, Science, and Technology, Japan, 2011–2015 [grant number S1101027].

Supplementary information

Supplementary information available online at
http://jcs.biologists.org/lookup/suppl/doi:10.1242/jcs.181883/-/DC1

References

Alderton, F., Rakhit, S., Kong, K. C., Palmer, T., Sambi, B., Pyne, S. and Pyne, N. J. (2001). Tethering of the platelet-derived growth factor beta receptor to G-protein-coupled receptors. A novel platform for integrative signaling by these receptor classes in mammalian cells. *J. Biol. Chem.* **276**, 28578-28585.

Ballmer-Hofer, K., Andersson, A. E., Ratcliffe, L. E. and Berger, P. (2011). Neuropilin-1 promotes VEGFR-2 trafficking through Rab11 vesicles thereby specifying signal output. *Blood* **118**, 816-826.

Blumer, J. B. and Lanier, S. M. (2014). Activators of G protein signaling exhibit broad functionality and define a distinct core signaling triad. *Mol. Pharmacol.* **85**, 388-396.

Ceresa, B. P. (2006). Regulation of EGFR endocytic trafficking by rab proteins. *Histol. Histopathol.* **21**, 987-993.

Cudmore, M. J., Hewett, P. W., Ahmad, S., Wang, K.-Q., Cai, M., Al-Ani, B., Fujisawa, T., Ma, B., Sissaoui, S., Ramma, W. et al. (2012). The role of heterodimerization between VEGFR-1 and VEGFR-2 in the regulation of endothelial cell homeostasis. *Nat. Commun.* **3**, 972.

Gourlaouen, M., Welti, J. C., Vasudev, N. S. and Reynolds, A. R. (2013). Essential role for endocytosis in the growth factor-stimulated activation of ERK1/2 in endothelial cells. *J. Biol. Chem.* **288**, 7467-7480.

Gu, S., Cifelli, C., Wang, S. and Heximer, S. P. (2009). RGS proteins: identifying new GAPs in the understanding of blood pressure regulation and cardiovascular function. *Clin. Sci.* **116**, 391-399.

Holmes, D. I. R. and Zachary, I. C. (2008). Vascular endothelial growth factor regulates stanniocalcin-1 expression via neuropilin-1-dependent regulation of KDR and synergism with fibroblast growth factor-2. *Cell. Signal.* **20**, 569-579.

Imamura, T., Vollenweider, P., Egawa, K., Clodi, M., Ishibashi, K., Nakashima, N., Ugi, S., Adams, J. W., Brown, J. H. and Olefsky, J. M. (1999). G alpha-q/11 protein plays a key role in insulin-induced glucose transport in 3T3-L1 adipocytes. *Mol. Cell. Biol.* **19**, 6765-6774.

Imoukhuede, P. I. and Popel, A. S. (2011). Quantification and cell-to-cell variation of vascular endothelial growth factor receptors. *Exp. Cell Res.* **317**, 955-965.

Imoukhuede, P. I., Dokun, A. O., Annex, B. H. and Popel, A. S. (2013). Endothelial cell-by-cell profiling reveals the temporal dynamics of VEGFR1 and VEGFR2 membrane localization after murine hindlimb ischemia. *Am. J. Physiol. Heart Circ. Physiol.* **304**, H1085-H1093.

Jopling, H. M., Odell, A. F., Hooper, N. M., Zachary, I. C., Walker, J. H. and Ponnambalam, S. (2009). Rab GTPase regulation of VEGFR2 trafficking and signaling in endothelial cells. *Arterioscler. Thromb. Vasc. Biol.* **29**, 1119-1124.

Jopling, H. M., Howell, G. J., Gamper, N. and Ponnambalam, S. (2011). The VEGFR2 receptor tyrosine kinase undergoes constitutive endosome-to-plasma membrane recycling. *Biochem. Biophys. Res. Commun.* **410**, 170-176.

Jopling, H. M., Odell, A. F., Pellet-Many, C., Latham, A. M., Frankel, P., Sivaprasadarao, A., Walker, J. H., Zachary, I. C. and Ponnambalam, S. (2014). Endosome-to-plasma membrane recycling of VEGFR2 receptor tyrosine kinase regulates endothelial function and blood vessel formation. *Cells* **3**, 363-385.

Kappert, K., Peters, K. G., Böhmer, F. D. and Ostman, A. (2005). Tyrosine phosphatases in vessel wall signaling. *Cardiovasc. Res.* **65**, 587-598.

Kimple, A. J., Bosch, D. E., Giguere, P. M. and Siderovski, D. P. (2011). Regulators of G-protein signaling and their Galpha substrates: promises and challenges in their use as drug discovery targets. *Pharmacol. Rev.* **63**, 728-749.

Kuemmerle, J. F. and Murthy, K. S. (2001). Coupling of the insulin-like growth factor-I receptor tyrosine kinase to Gi2 in human intestinal smooth muscle: Gbetagamma-dependent mitogen-activated protein kinase activation and growth. *J. Biol. Chem.* **276**, 7187-7194.

Lamalice, L., Houle, F. and Huot, J. (2006). Phosphorylation of Tyr 1214 within VEGFR-2 triggers the recruitment of Nck and activation of Fyn leading to SAPK2/p38 activation and endothelial cell migration in response to VEGF. *J. Biol. Chem.* **281**, 34009-34020.

Lehmann, D. M., Seneviratne, A. M. P. B. and Smrcka, A. V. (2008). Small molecule disruption of G protein beta gamma subunit signaling inhibits neutrophil chemotaxis and inflammation. *Mol. Pharmacol.* **73**, 410-418.

Leung, T., Chen, H., Stauffer, A. M., Giger, K. E., Sinha, S., Horstick, E. J., Humbert, J. E., Hansen, C. A. and Robishaw, J. D. (2006). Zebrafish G protein gamma2 is required for VEGF signaling during angiogenesis. *Blood* **108**, 160-166.

Manickam, V., Tiwari, A., Jung, J.-J., Bhattacharya, R., Goel, A., Mukhopadhyay, D. and Choudhury, A. (2011). Regulation of vascular endothelial growth factor receptor 2 trafficking and angiogenesis by Golgi localized t-SNARE syntaxin 6. *Blood* **117**, 1425-1435.

Marti, H. H. and Risau, W. (1998). Systemic hypoxia changes the organ-specific distribution of vascular endothelial growth factor and its receptors. *Proc. Natl. Acad. Sci. USA* **95**, 15809-15814.

Nisancioglu, M. H., Mahoney, W. M., Jr, Kimmel, D. D., Schwartz, S. M., Betsholtz, C. and Genove, G. (2008). Generation and characterization of rgs5 mutant mice. *Mol. Cell. Biol.* **28**, 2324-2331.

Pellet-Many, C., Frankel, P., Jia, H. and Zachary, I. (2008). Neuropilins: structure, function and role in disease. *Biochem. J.* **411**, 211-226.

Roskoski, R. (2008). VEGF receptor protein–tyrosine kinases: structure and regulation. *Biochem. Biophys. Res. Commun.* **375**, 287-291.

Sato, M. (2013). Roles of accessory proteins for heterotrimeric g-protein in the development of cardiovascular diseases. *Circ. J.* **77**, 2455-2461.

Sato, M., Kataoka, R., Dingus, J., Wilcox, M., Hildebrandt, J. D. and Lanier, S. M. (1995). Factors determining specificity of signal transduction by G-protein-coupled receptors: regulation of signal transfer from receptor to G-protein. *J. Biol. Chem.* **270**, 15269-15276.

Sato, M., Gettys, T. W. and Lanier, S. M. (2004). AGS3 and signal integration by Galpha(s)- and Galpha(i)-coupled receptors: AGS3 blocks the sensitization of adenylyl cyclase following prolonged stimulation of a Galpha(i)-coupled receptor by influencing processing of Galpha(i). *J. Biol. Chem.* **279**, 13375-13382.

Sato, M., Blumer, J. B., Simon, V. and Lanier, S. M. (2006a). Accessory proteins for G proteins: partners in signaling. *Annu. Rev. Pharmacol. Toxicol.* **46**, 151-187.

Sato, M., Cismowski, M. J., Toyota, E., Smrcka, A. V., Lucchesi, P. A., Chilian, W. M. and Lanier, S. M. (2006b). Identification of a receptor-independent activator of G protein signaling (AGS8) in ischemic heart and its interaction with Gbetagamma. *Proc. Natl. Acad. Sci. USA* **103**, 797-802.

Sato, M., Jiao, Q., Honda, T., Kurotani, R., Toyota, E., Okumura, S., Takeya, T., Minamisawa, S., Lanier, S. M. and Ishikawa, Y. (2009). Activator of G protein signaling 8 (AGS8) is required for hypoxia-induced apoptosis of cardiomyocytes: role of G betagamma and connexin 43 (CX43). *J. Biol. Chem.* **284**, 31431-31440.

Sato, M., Hiraoka, M., Suzuki, H., Bai, Y., Kurotani, R., Yokoyama, U., Okumura, S., Cismowski, M. J., Lanier, S. M. and Ishikawa, Y. (2011). Identification of transcription factor E3 (TFE3) as a receptor-independent activator of Galpha16: gene regulation by nuclear Galpha subunit and its activator. *J. Biol. Chem.* **286**, 17766-17776.

Sato, M., Hiraoka, M., Suzuki, H., Sakima, M., Mamun, A. A., Yamane, Y., Fujita, T., Yokoyama, U., Okumura, S. and Ishikawa, Y. (2014). Protection of cardiomyocytes from the hypoxia-mediated injury by a peptide targeting the activator of G-protein signaling 8. *PLoS ONE* **9**, e91980.

Schneider, C. A., Rasband, W. S. and Eliceiri, K. W. (2012). NIH Image to ImageJ: 25 years of image analysis. *Nat. Methods* **9**, 671-675.

Silini, A., Ghilardi, C., Figini, S., Sangalli, F., Fruscio, R., Dahse, R., Pedley, R. B., Giavazzi, R. and Bani, M. (2012). Regulator of G-protein signaling 5 (RGS5) protein: a novel marker of cancer vasculature elicited and sustained by the tumor's proangiogenic microenvironment. *Cell. Mol. Life Sci.* **69**, 1167-1178.

Ulyatt, C., Walker, J. and Ponnambalam, S. (2011). Hypoxia differentially regulates VEGFR1 and VEGFR2 levels and alters intracellular signaling and

cell migration in endothelial cells. *Biochem. Biophys. Res. Commun.* **404**, 774-779.

Wieland, T. and Mittmann, C. (2003). Regulators of G-protein signalling: multifunctional proteins with impact on signalling in the cardiovascular system. *Pharmacol. Ther.* **97**, 95-115.

Zeng, H., Zhao, D. and Mukhopadhyay, D. (2002). Flt-1-mediated down-regulation of endothelial cell proliferation through pertussis toxin-sensitive G proteins, beta gamma subunits, small GTPase CDC42, and partly by Rac-1. *J. Biol. Chem.* **277**, 4003-4009.

Zeng, H., Zhao, D., Yang, S., Datta, K. and Mukhopadhyay, D. (2003). Heterotrimeric G alpha q/G alpha 11 proteins function upstream of vascular endothelial growth factor (VEGF) receptor-2 (KDR) phosphorylation in vascular permeability factor/VEGF signaling. *J. Biol. Chem.* **278**, 20738-20745.

Zhang, P. and Mende, U. (2011). Regulators of G-protein signaling in the heart and their potential as therapeutic targets. *Circ. Res.* **109**, 320-333.

Zhou, J., Moroi, K., Nishiyama, M., Usui, H., Seki, N., Ishida, J., Fukamizu, A. and Kimura, S. (2001). Characterization of RGS5 in regulation of G protein-coupled receptor signaling. *Life Sci.* **68**, 1457-1469.